COMMUN. MATH. SCI.
Vol. 16, No. 3, pp. 857–877

THE DIRECT AND INVERSE ELASTIC SCATTERING PROBLEMS FOR TWO SCATTERERS IN CONTACT*

JUN GUO[†], HAO WU[‡], AND LEI XIAO[§]

Abstract. This paper is concerned with the elastic scattering problem of a combined scatterer, which consists of a penetrable obstacle and a hard crack touching with each other. By using the boundary integral equation method, the direct scattering problem is formulated as a boundary integral system, then we obtain the existence and uniqueness of a weak solution according to Fredholm theory. The inverse scattering problem we are dealing with is the shape reconstruction of the combined scatterer from the knowledge of far field patterns due to the incident plane compressional and shear waves. Based on an analysis of a particular transmission eigenvalue problem, the linear sampling method is established to reconstruct the combined scatterer. The numerical experiments show the feasibility and validity of the proposed method.

Keywords. elastic scattering; combined scatterer; linear sampling method.

AMS subject classifications. 35R30; 35Q30.

1. Introduction

The scattering problems of elastic wave by obstacles have attracted great attention and a lot of achievements have been made for different kinds of obstacle scattering. Usually, it can be classified into rigid scatterers, cavities, penetrable bodies and cracks. However, the scatterers may be in contact with each other in practical situation. In this paper, we consider the elastic scattering of a combined scatterer, which is composed of a penetrable obstacle and a hard crack in contact. Thus the elastic wave transmits to the interior of the obstacle from the untouched part of the boundary.

Specifically, assume that the penetrable obstacle occupy a bounded domain $D_i \subset \mathbb{R}^2$, with smooth boundary ∂D_i, and let the open smooth curve $\Sigma \subset \mathbb{R}^2$ denote the hard crack. The unbounded domain $\mathbb{R}^2 \backslash (\overline{D}_i \cup \overline{\Sigma})$ is denoted by D_e. We assume that an obstacle is located on the crack, the contacted portion of the boundary ∂D_i is denoted by Γ_2, the other is denoted by Γ_1. Furthermore, we assume that the crack can be extended to a closed smooth curve $\partial\Omega$ including a bounded domain Ω, such that $D_i \subset \Omega$. Both domains of D_i and D_e are occupied by isotropic and homogeneous elastic medium with constant density ρ_α, Lamé constants μ_α and λ_α satisfying $\mu_\alpha > 0, 2\mu_\alpha + \lambda_\alpha > 0$, for $\alpha = i,e$. The curves Γ_1 and Σ do not form a cusp, so that D_i, $\Omega \backslash \overline{D_i}$ and D_e are all Lipschitz domains. Then the scattering of time harmonic elastic plane wave $\mathbf{u}^{in}$ by the combined scatterer excites the scattered wave $\mathbf{u}$ in D_e and transmitted wave $\mathbf{v}$ in D_i, which are governed by the Navier equation

$$\begin{cases} \mu_e \Delta \mathbf{u} + (\mu_e + \lambda_e) \nabla (\nabla \cdot \mathbf{u}) + \rho_e \omega^2 \mathbf{u} = \mathbf{0} & \text{in } D_e, \\ \mu_i \Delta \mathbf{v} + (\mu_i + \lambda_i) \nabla (\nabla \cdot \mathbf{v}) + \rho_i \omega^2 \mathbf{v} = \mathbf{0} & \text{in } D_i, \end{cases} \tag{1.1}$$

*Received: September 24, 2017; accepted (in revised form): February 26, 2018. Communicated by Liliana Borcea.
This research is supported by National Natural Science Foundation of People's Republic of China, No. 11571132, and the Fundamental Research Funds for South-Central University for Nationalities, No. CZT18010.
[†]School of Mathematics and Statistics, South-Central University For Nationalities, Wuhan, P.R. China (hssxgj@126.com).
[‡]School of Mathematics and Statistics, South-Central University For Nationalities, Wuhan, P.R. China (wuhaomoonsky@163.com).
[§]Corresponding author, School of Statistics and Mathematics, Zhongnan University of Economics and Law, Wuhan, P.R. China (xiaoleiyouhua@sina.com).

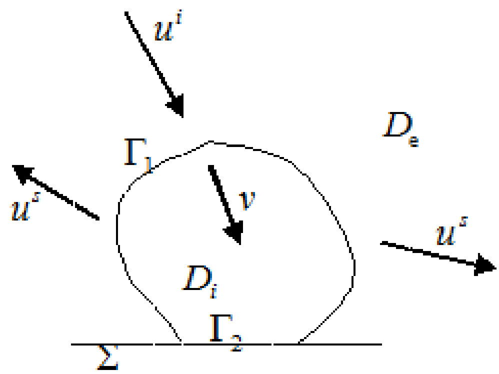

FIG. 1.1. *The penetrable isotropic and homogeneous elastic obstacle D_i, which is situated on a hard crack Σ, is illuminated by the elastic plane wave $\mathbf{u}^{in}$. The transmitted wave in D_i is denoted by $\mathbf{v}$ and the scattered wave in D_e is denoted by $\mathbf{u}$*

where $\omega > 0$ is the circular frequency. Hereafter, we will denote by Δ_α^* the Lamé operator $\mu_\alpha\Delta + (\mu_\alpha + \lambda_\alpha)\nabla(\nabla\cdot)$ for brevity. The total displacement field $\mathbf{u}^t$ is the superposition of the incident filed $\mathbf{u}^{in}$ and the scattered field $\mathbf{u}$, i.e., $\mathbf{u}^t = \mathbf{u}^{in} + \mathbf{u}$. The scattering configuration is shown in Figure 1.1.

A description of some notations is given as follows. For $\mathbf{x} \in \mathbb{R}^2$, let $\hat{\mathbf{x}}$ be the unit vector $\hat{\mathbf{x}} := \mathbf{x}/|\mathbf{x}|$ and $\mathbf{x}^\perp$ be the vector obtained by rotating $\mathbf{x}$ anticlockwise by $\pi/2$. As usual, we use the notations $\mathbf{a}\cdot\mathbf{b}$ to represent the scalar product and $\mathbf{a}\times\mathbf{b}$ to present the vector product for $\mathbf{a},\mathbf{b} \in \mathbb{R}^2$. For a vector function $\mathbf{u} = [u^1, u^2]^\top$ and a matrix function $W = [\mathbf{w}^1, \mathbf{w}^2]^\top$, the symbols $\nabla\mathbf{u}$ and $\nabla\cdot W$ are denoted respectively by

$$\nabla\mathbf{u} = [\nabla u^1, \nabla u^2]^\top, \quad \nabla\cdot W = [\nabla\cdot\mathbf{w}^1, \nabla\cdot\mathbf{w}^2]^\top.$$

Let $\mathbf{n}$ be the unit outward normal vector of the boundaries ∂D_i and $\partial\Omega$. The following transmission boundary conditions are satisfied on the penetrable part of the boundary ∂D_i

$$\begin{cases} \mathbf{u} + \mathbf{u}^{in} = \mathbf{v} & \text{on } \Gamma_1, \\ T_e\mathbf{u} + T_e\mathbf{u}^{in} = T_i\mathbf{v} & \text{on } \Gamma_1. \end{cases} \tag{1.2}$$

Here, T_α is the surface stress operator on Γ_1 which is given by

$$\begin{aligned} T_\alpha\mathbf{w} &= (2\mu_\alpha\mathbf{n}\cdot\nabla + \lambda_\alpha\mathbf{n}\nabla\cdot - \mu_\alpha\mathbf{n}^\perp\nabla^\perp\cdot)\mathbf{w} \\ &= \begin{bmatrix} (\lambda_\alpha + 2\mu_\alpha)\dfrac{\partial w_1}{\partial x_1} + \lambda_\alpha\dfrac{\partial w_2}{\partial x_2} & \mu_\alpha(\dfrac{\partial w_1}{\partial x_2} + \dfrac{\partial w_2}{\partial x_1}) \\ \mu_\alpha(\dfrac{\partial w_1}{\partial x_2} + \dfrac{\partial w_2}{\partial x_1}) & \lambda_\alpha\dfrac{\partial w_1}{\partial x_1} + (\lambda_\alpha + 2\mu_\alpha)\dfrac{\partial w_2}{\partial x_2} \end{bmatrix}\mathbf{n}. \end{aligned}$$

We impose the Dirichlet boundary condition on the touching part Γ_2 and on the crack Σ, respectively for $\mathbf{v}$ and $\mathbf{u}$.

$$\mathbf{v} = \mathbf{0} \quad \text{on } \Gamma_2. \tag{1.3}$$

$$\mathbf{u}+\mathbf{u}^{in}=\mathbf{0} \quad \text{on } \Sigma. \tag{1.4}$$

Assume that the incident wave is given by either a longitudinal plane wave with the form

$$\mathbf{u}^{in}=\mathbf{u}_p^{in}=\mathbf{d}e^{ik_{p,e}\mathbf{x}\cdot\mathbf{d}}, \quad \mathbf{d}\in\mathbb{S}$$

where $\mathbb{S}$ is the unit circle in $\mathbb{R}^2$ and $\mathbf{d}$ is the incident direction, or a transversal plane wave with the form

$$\mathbf{u}^{in}=\mathbf{u}_s^{in}=\mathbf{q}e^{ik_{s,e}\mathbf{x}\cdot\mathbf{d}}, \quad \mathbf{q},\mathbf{d}\in\mathbb{S}$$

where $\mathbf{q}$ is the polarization direction such that $\mathbf{q}\perp\mathbf{d}$. The wave numbers of compressional and shear waves $k_{p,e}$ and $k_{s,e}$, respectively are given by

$$k_{p,e}=\omega\sqrt{\frac{\rho_e}{2\mu_e+\lambda_e}} \quad \text{and} \quad k_{s,e}=\omega\sqrt{\frac{\rho_e}{\mu_e}}.$$

The wave numbers $k_{p,i}$ and $k_{s,i}$ can be defined by a similar way.

By the Helmholtz decomposition theorem [1], the scattered field $\mathbf{u}$ can be decomposed as

$$\mathbf{u}=\mathbf{u}_p+\mathbf{u}_s, \quad \mathbf{u}_p=-\frac{1}{k_{p,e}^2}\nabla(\nabla\cdot\mathbf{u}), \quad \mathbf{u}_s=-\frac{1}{k_{s,e}^2}\nabla^\perp(\nabla^\perp\cdot\mathbf{u})$$

where $\mathbf{u}_p$ denotes the longitudinal wave and $\mathbf{u}_s$ is the transversal wave. It is well known that $\mathbf{u}_a(a=p,s)$ satisfies the Helmholtz equation

$$\Delta\mathbf{u}_a+k_{a,e}^2\mathbf{u}_a=\mathbf{0}.$$

In addition, each displacement field $\mathbf{u}$ has to satisfy the Kupradze radiation condition [2]

$$\lim_{r\to\infty}\sqrt{r}\Big(\frac{\partial\mathbf{u}_p}{\partial r}-ik_{p,e}\mathbf{u}_p\Big)=\mathbf{0}, \quad \lim_{r\to\infty}\sqrt{r}\Big(\frac{\partial\mathbf{u}_s}{\partial r}-ik_{s,e}\mathbf{u}_s\Big)=\mathbf{0}, \quad r=|\mathbf{x}| \tag{1.5}$$

uniformly in all direction $\hat{\mathbf{x}}\in\mathbb{S}$. In other words, both of the compressional and shear wave fields satisfy the Sommerfeld radiation condition. Throughout this paper, the solution of Navier Equation (1.1) satisfying the Kupradze radiation condition is called the radiating solution. It is hold that the radiating solution to the Navier equation has the asymptotic expansions of the forms [3, 4]

$$\mathbf{u}(\mathbf{x})=\frac{e^{ik_{p,e}|\mathbf{x}|}}{\sqrt{|\mathbf{x}|}}u_p^\infty(\hat{\mathbf{x}})\hat{\mathbf{x}}+\frac{e^{ik_{s,e}|\mathbf{x}|}}{\sqrt{|\mathbf{x}|}}u_s^\infty(\hat{\mathbf{x}})\hat{\mathbf{x}}^\perp+O(|\mathbf{x}|^{-3/2}), \quad |\mathbf{x}|\to\infty \tag{1.6}$$

and

$$T_{e,\hat{\mathbf{x}}}\mathbf{u}(\mathbf{x})=\frac{i\omega^2}{k_{p,e}}\frac{e^{ik_{p,e}|\mathbf{x}|}}{\sqrt{|\mathbf{x}|}}u_p^\infty(\hat{\mathbf{x}})\hat{\mathbf{x}}+\frac{i\omega^2}{k_{s,e}}\frac{e^{ik_{s,e}|\mathbf{x}|}}{\sqrt{|\mathbf{x}|}}u_s^\infty(\hat{\mathbf{x}})\hat{\mathbf{x}}^\perp+O(|\mathbf{x}|^{-1}), \quad |\mathbf{x}|\to\infty, \tag{1.7}$$

where $u_p^\infty(\hat{\mathbf{x}})$ is the compressional far field pattern of $\mathbf{u}$ and $u_s^\infty(\hat{\mathbf{x}})$ is the shear far field pattern of $\mathbf{u}$. The far field pattern of the scattered field $\mathbf{u}$ is defined by

$$\mathbf{u}^\infty(\hat{\mathbf{x}}) = (u_p^\infty(\hat{\mathbf{x}}), u_s^\infty(\hat{\mathbf{x}})).$$

The direct scattering problem (1.1)–(1.5) is regarded as **DP**, and the classical boundary integral equation method will be used to solve it since no related result can be found. An equivalent boundary integral system of the first kind containing strongly singular and hypersingular kernels is deduced, and based on the strong ellipticity theorem [10], the existence and uniqueness of the solution is obtained. We mention that there are some results by applying the boundary integral equation method to solve elastic crack scattering problems (see for examples [5–7]) and the elastic obstacle scattering problems (see for examples [3, 8, 9, 11]).

For the inverse scattering problem, we are interested in the determination of the crack Σ and obstacle D_i. This problem will be called **IP**. The inversion data is the knowledge of the far field pattern $\mathbf{u}^\infty(\hat{\mathbf{x}}, \mathbf{d}; \mathbf{t})$ of the scattering field $\mathbf{u}(\mathbf{x}, \mathbf{d}; \mathbf{t})$ for the following: all observation direction $\hat{\mathbf{x}} \in \mathbb{S}$, incident direction $\mathbf{d} \in \mathbb{S}$ and the polarization $\mathbf{t} = \mathbf{d}$ or $\mathbf{q}$ associated with the incident plane wave $\mathbf{d}e^{ik_{p,e}\mathbf{x}\cdot\mathbf{d}}$ or $\mathbf{q}e^{ik_{s,e}\mathbf{x}\cdot\mathbf{d}}$. We aim at extending the linear sampling method to the inverse elastic scattering problems **IP**.

The linear sampling method was first introduced by Colton and Kirsch [12] to solve inverse acoustic scattering problem in 1996. Since then it has been well studied and proved to be an excellent method for inverse shape problems in acoustic, electromagnetic, elastic scattering, electrical impedance tomography, as well as been developed in time dependent partial differential equation. This approach has attracted so much attention because no a priori information concerning geometry and boundary conditions of the scattering obstacle is required and the numerical implementation is really simple. See [13, 14] for the mathematical foundations of this method, refer to the book [15] for a good understanding and survey, and recommend the papers [16, 17] for a new development.

Historically, Arens firstly applied the linear sampling method for inverse elastic scattering problem [18] to two-dimensional elastic scattering for the rigid body problem. The rigid bodies or cavities in three dimensions are given in [19]. The elastic transmission scattering problems for isotropic and anisotropic elastic media can be found in [20–22]. Finally, we mention that the near field linear sampling method is adopted to deal with the reconstruction of elastic scatterers in semi-infinite solid [23] and the inverse fluid–solid problem [24].

All of the aforementioned works treat with single obstacle or multiple scatterers with the same properties. However, the mixed type scatterers may appear in the actual applied Science, and this kind of inverse scattering problem has received a number of research results. In 2004, Grinberg and Kirsch [25] considered a multiple scattering problem and established the factorization method in the case when sound-soft and sound-hard scatterers are a priori geometrically separated. In 2013, Kirsch and Liu [30] studied the factorization method for recovering the location and shape of the mixed type scatterer–a bounded impenetrable obstacle and a penetrable inhomogeneous medium with compact support and later developed by the author Liu [31] for the union of impenetrable and penetrable scatterers with different physical properties. For more relevant results, please refer to [27–29] and [32], and to monograph [26] for a comprehensive study of the multiple scattering in general.

Nevertheless, the direct and inverse scattering problems for mixed type scatterers in contact with each other are rarely reported. The purpose of this paper is to make some effort on such issue and seek the solutions to direct elastic scattering problem **DP** and inverse elastic scattering problem **IP**. A similar acoustic scattering problem has been considered in [33], where the undetermined obstacle touches a known perfect thin conductor and the linear sampling method is proposed to reconstruct the shape and location of the obstacle from near field measurements. The under consideration is different in two aspects: on one hand, we want to completely show the well posedness of direct scattering problem, on the other, we want to simultaneously recover the obstacle and the crack from far field data.

The outline of this paper is organized as follows. In Section 2, using the boundary integral equation approach, an equivalent boundary integral system is deduced and the Fredholm property of the related operator is proved by the Fredholm theorem. Therefore the solvability of the problem **DP** is established. Section 3 gives a rigorous proof of the linear sampling method for the reconstruction of the combined scatterer. As usual in transmission problems, a special interior transmission problem needs to be discussed in order to guarantee the injectivity of the far field operator. The numerical experiments will be presented in Section 4 to demonstrate the correctness and effectiveness of the proposed method.

2. The direct scattering problem

This section is concern with the direct scattering problem **DP**. Recall that the open arc Σ belongs to a closed curve $\partial\Omega$ surrounding a bounded domain Ω. Let $H^1(\Omega)$ and $H^1_{loc}(\mathbb{R}^2\backslash\overline{\Omega})$ be the usual Sobolev spaces with $H^{1/2}(\partial\Omega)$ being the trace space. We introduce the following trace spaces on Σ.

$$
\begin{aligned}
&[H^{1/2}(\Sigma)]^2=\{\mathbf{u}|_\Sigma:\ \mathbf{u}\in[H^{1/2}(\partial\Omega)]^2\},\\
&[\widetilde{H}^{1/2}(\Sigma)]^2=\{\mathbf{u}\in[H^{1/2}(\partial\Omega)]^2:\ \mathrm{supp}\,\mathbf{u}\subseteq\overline{\Sigma}\},\\
&[H^{-1/2}(\Sigma)]^2=\Big([\widetilde{H}^{1/2}(\Sigma)]^2\Big)',\ \text{the dual space of } [\widetilde{H}^{1/2}(\Sigma)]^2,\\
&[\widetilde{H}^{-1/2}(\Sigma)]^2=\Big([H^{1/2}(\Sigma)]^2\Big)',\ \text{the dual space of } [H^{1/2}(\Sigma)]^2.
\end{aligned}
$$

Let us consider a general problem: Assume $\mathbf{f}\in[H^{1/2}(\Gamma_1)]^2$, $\mathbf{g}\in[H^{-1/2}(\Gamma_1)]^2$ and $\mathbf{h}\in[H^{1/2}(\Sigma)]^2$ seek a radiating solution $\mathbf{u}\in[H^1_{loc}(D_e)]^2$ and $\mathbf{v}\in[H^1(D_i)]^2$ such that

$$
\begin{cases}
\Delta_e^*\mathbf{u}+\rho_e\omega^2\mathbf{u} &=\mathbf{0}\quad \text{in } D_e,\\
\Delta_i^*\mathbf{v}+\rho_i\omega^2\mathbf{v} &=\mathbf{0}\quad \text{in } D_i,\\
\mathbf{u}-\mathbf{v} &=\mathbf{f}\quad \text{on } \Gamma_1,\\
T_e\mathbf{u}-T_i\mathbf{v} &=\mathbf{g}\quad \text{on } \Gamma_1,\\
\mathbf{v} &=\mathbf{0}\quad \text{on } \Gamma_2,\\
\mathbf{u} &=\mathbf{h}\quad \text{on } \Sigma.
\end{cases}
\tag{2.1}
$$

LEMMA 2.1. *The problem (2.1) has at most one solution.*

Proof. Assume that $(\mathbf{u},\mathbf{v})$ be a solution pair to the homogeneous boundary value problem (2.1). For two vector fields $\mathbf{p},\mathbf{q}\in[H^1(D)]^2$, where $D\subset\mathbb{R}^2$ is a bounded and smooth domain, let $E_\alpha(\mathbf{p},\mathbf{q})$ be given as

$$
\begin{aligned}
E_\alpha(\mathbf{p},\mathbf{q})=(2\mu_\alpha+\lambda_\alpha)\Big(\frac{\partial p_1}{\partial x_1}\frac{\partial q_1}{\partial x_1}+\frac{\partial p_2}{\partial x_2}\frac{\partial q_2}{\partial x_2}\Big)+\mu_\alpha\Big(\frac{\partial p_1}{\partial x_2}\frac{\partial q_1}{\partial x_2}+\frac{\partial p_2}{\partial x_1}\frac{\partial q_2}{\partial x_1}\Big)\\
+\lambda_\alpha\Big(\frac{\partial p_1}{\partial x_1}\frac{\partial q_2}{\partial x_2}+\frac{\partial p_2}{\partial x_2}\frac{\partial q_1}{\partial x_1}\Big)+\mu_\alpha\Big(\frac{\partial p_1}{\partial x_2}\frac{\partial q_2}{\partial x_1}+\frac{\partial p_2}{\partial x_1}\frac{\partial q_1}{\partial x_2}\Big).
\end{aligned}
$$

Then for a circle B_r center at the origin, with radius r large enough such that $D_i\cup\overline{\Sigma}$ is included in, Betti's first formula [2] in the domain $D_e\cap B_r$ for $\mathbf{u}$ and $\overline{\mathbf{u}}$ yields that by noting the boundary condition on Σ in (2.1):

$$\int_{B_r\cap D_e} E_e(\mathbf{u},\overline{\mathbf{u}})d\mathbf{x}-\int_{B_r\cap D_e}\rho_e\omega^2|\mathbf{u}|^2d\mathbf{x}=\int_{\partial B_r}T_e\mathbf{u}\cdot\overline{\mathbf{u}}ds-\int_{\Gamma_1}T_e\mathbf{u}\cdot\overline{\mathbf{u}}ds.$$

Analogously, using the boundary condition on Γ_2, we obtain the following for $\mathbf{v}$ in the domain D_i.

$$\int_{D_i}E_i(\mathbf{v},\overline{\mathbf{v}})d\mathbf{x}-\int_{D_i}\rho_i\omega^2|\mathbf{v}|^2d\mathbf{x}=\int_{\Gamma_1}T_i\mathbf{v}\cdot\overline{\mathbf{v}}ds.$$

The sum of the above two identities and the transmission boundary conditions on Γ_1 show that

$$\int_{B_r\cap D_e}\left\{E_e(\mathbf{u},\overline{\mathbf{u}})-\rho_e\omega^2|\mathbf{u}|^2\right\}d\mathbf{x}+\int_{D_i}\left\{E_i(\mathbf{v},\overline{\mathbf{v}})-\rho_i\omega^2|\mathbf{v}|^2\right\}d\mathbf{x}=\int_{\partial B_r}T_e\mathbf{u}\cdot\overline{\mathbf{u}}ds. \tag{2.2}$$

Using the orthogonality of the compressional and the shear far field pattern, we have that from the asymptotic representations (1.6) and (1.7)

$$T_{e,\hat{\mathbf{x}}}\mathbf{u}\cdot\overline{\mathbf{u}}=\frac{i\omega^2}{k_{p,e}r}|u_p^\infty(\hat{\mathbf{x}})|^2+\frac{i\omega^2}{k_{s,e}r}|u_s^\infty(\hat{\mathbf{x}})|^2+O(|r|^{-5/2}).$$

Since $ImE_e(\mathbf{u},\overline{\mathbf{u}})=0$ and $ImE_i(\mathbf{v},\overline{\mathbf{v}})=0$, taking the imaginary part of equation (2.2) we arrive at $u_p^\infty(\hat{\mathbf{x}})=0$ and $u_s^\infty(\hat{\mathbf{x}})=0$. Thus we obtain that $\mathbf{u}_p=\mathbf{0}$ and $\mathbf{u}_s=\mathbf{0}$ in D_e by Rellich's lemma [34]. The transmission boundary conditions and Holmgren's uniqueness theorem indicate that $\mathbf{v}=\mathbf{0}$ in D_i. The proof is thus completed. □

We now introduce the fundamental solution, also called Green's tensor of the Navier equation in free space, which is given by

$$\Gamma_\alpha(\mathbf{x},\mathbf{y})=\frac{i}{4\mu}H_0^{(1)}(k_{s,\alpha}|\mathbf{x}-\mathbf{y}|)I+\frac{i}{4\omega^2}\nabla_x^\top\nabla_x(H_0^{(1)}(k_{s,\alpha}|\mathbf{x}-\mathbf{y}|)-H_0^{(1)}(k_{p,\alpha}|\mathbf{x}-\mathbf{y}|))$$

for $\mathbf{x},\mathbf{y}\in\mathbb{R}^2$ and $\mathbf{x}\neq\mathbf{y}$, where $H_0^{(1)}(\cdot)$ is the Hankel function of the first kind of order zero.

In what follows, to facilitate the description of the notations, we denote by Γ_3 the open curve Σ. The four boundary integral operators in terms of the fundamental solution will be used

$$\begin{aligned}
(H_{jl}^\alpha\mathbf{g})(\mathbf{x})&=\int_{\Gamma_j}\Gamma_\alpha(\mathbf{x},\mathbf{y})\mathbf{g}(\mathbf{y})ds(\mathbf{y}), && \mathbf{x}\in\Gamma_l,\\
(K_{jl}^\alpha\mathbf{g})(\mathbf{x})&=\int_{\Gamma_j}[T_{\alpha,\mathbf{y}}\Gamma_\alpha(\mathbf{x},\mathbf{y})]^\top\mathbf{g}(\mathbf{y})ds(\mathbf{y}), && \mathbf{x}\in\Gamma_l,\\
(K_{jl}^{'\alpha}\mathbf{g})(\mathbf{x})&=\int_{\Gamma_j}T_{\alpha,\mathbf{x}}\Gamma_\alpha(\mathbf{x},\mathbf{y})\mathbf{g}(\mathbf{y})ds(\mathbf{y}), && \mathbf{x}\in\Gamma_l,\\
(L_{jl}^\alpha\mathbf{g})(\mathbf{x})&=T_{\alpha,\mathbf{x}}\int_{\Gamma_j}[T_{\alpha,\mathbf{y}}\Gamma_\alpha(\mathbf{x},\mathbf{y})]^\top\mathbf{g}(\mathbf{y})ds(\mathbf{y}), && \mathbf{x}\in\Gamma_l,
\end{aligned}$$

for $j,l=1,2,3$. They possess the mapping properties (see Chapter 6 in [10])

$$H_{ll}^\alpha:[\widetilde{H}^{-1/2}(\Gamma_l)]^2\to[H^{1/2}(\Gamma_l)]^2,\qquad K_{ll}^\alpha:[\widetilde{H}^{1/2}(\Gamma_l)]^2\to[H^{1/2}(\Gamma_l)]^2,$$

$$K_{ll}^{\prime\alpha}:[\widetilde{H}^{-1/2}(\Gamma_l)]^2\to[H^{-1/2}(\Gamma_l)]^2,\qquad L_{ll}^{\alpha}:[\widetilde{H}^{1/2}(\Gamma_l)]^2\to[H^{-1/2}(\Gamma_l)]^2.$$

REMARK 2.1. Note that for density in Sobolev spaces with negative exponent, the boundary integral operators are understood in general sense. For the sake of consistency, we still call them boundary integral operators in this paper.

Next we will use the layer potentials to reformulate the problem (2.1) and seek the solution pair $(\mathbf{u},\mathbf{v})$ in the form of combined single-and double-layer potentials

$$\mathbf{u}(\mathbf{x})=\int_{\Gamma_1}\Big\{\Gamma_e(\mathbf{x},\mathbf{y})\mathbf{a}(\mathbf{y})-[T_{e,\mathbf{y}}\Gamma_e(\mathbf{x},\mathbf{y})]^\top\mathbf{b}(\mathbf{y})\Big\}ds(\mathbf{y})+\int_{\Gamma_3}\Gamma_e(\mathbf{x},\mathbf{y})\mathbf{e}(\mathbf{y})ds(\mathbf{y}),\ \mathbf{x}\in D_e. \tag{2.3}$$

$$\mathbf{v}(\mathbf{x})=\int_{\Gamma_1}\Big\{[T_{i,\mathbf{y}}\Gamma_i(\mathbf{x},\mathbf{y})]^\top\mathbf{b}(\mathbf{y})-\Gamma_i(\mathbf{x},\mathbf{y})\mathbf{a}(\mathbf{y})\Big\}ds(\mathbf{y})+\int_{\Gamma_2}\Gamma_i(\mathbf{x},\mathbf{y})\mathbf{c}(\mathbf{y})ds(\mathbf{y}),\ \mathbf{x}\in D_i. \tag{2.4}$$

Here $\mathbf{a}\in[\widetilde{H}^{-1/2}(\Gamma_1)]^2$, $\mathbf{b}\in[\widetilde{H}^{1/2}(\Gamma_1)]^2$, $\mathbf{c}\in[\widetilde{H}^{-1/2}(\Gamma_2)]^2$ and $\mathbf{e}\in[\widetilde{H}^{-1/2}(\Gamma_3)]^2$ are the undetermined densities. Note that the single-and double-layer potentials with such functions ensure that $(\mathbf{u},\mathbf{v})$ belongs to $[H^1_{loc}(D_e)]^2\times[H^1(D_i)]^2$.

By the well known jump relations of single-and double-layer potentials [10], we obtain a boundary integral system from the boundary conditions in Equation (2.1)

$$\begin{bmatrix} H_{11}^e+H_{11}^i & -K_{11}^e-K_{11}^i & -H_{21}^i & H_{31}^e\\ K_{11}^{\prime e}+K_{11}^{\prime i} & -L_{11}^e-L_{11}^i & -K_{21}^{\prime i} & K_{31}^{\prime e}\\ -H_{12}^i & K_{12}^i & H_{22}^i & 0\\ H_{13}^e & -K_{13}^e & 0 & H_{33}^e\end{bmatrix}\begin{bmatrix}\mathbf{a}\\ \mathbf{b}\\ \mathbf{c}\\ \mathbf{e}\end{bmatrix}=\begin{bmatrix}\mathbf{f}\\ \mathbf{g}\\ \mathbf{0}\\ \mathbf{h}\end{bmatrix}. \tag{2.5}$$

Denote by M the boundary integral operator appearing on the left side of above equation, and define the Sobolev spaces

$$X:=[\widetilde{H}^{-1/2}(\Gamma_1)]^2\times[\widetilde{H}^{1/2}(\Gamma_1)]^2\times[\widetilde{H}^{-1/2}(\Gamma_2)]^2\times[\widetilde{H}^{-1/2}(\Gamma_3)]^2,$$

$$X^*:=[H^{1/2}(\Gamma_1)]^2\times[H^{-1/2}(\Gamma_1)]^2\times[H^{1/2}(\Gamma_2)]^2\times[H^{1/2}(\Gamma_3)]^2,$$

We can to observe that $M:X\to X^*$ is bounded.

Next we show the solvability of the integral system (2.5).

LEMMA 2.2. *The operator $M:X\to X^*$ is a Fredholm operator with index zero.*

Proof. Extend $\mathbf{a}$, $\mathbf{b}$ and $\mathbf{c}$ to the whole boundary ∂D_i by zero and denote them by $\widetilde{\mathbf{a}}\in[H^{-1/2}(\partial D_i)]^2$, $\widetilde{\mathbf{b}}\in[H^{1/2}(\partial D_i)]^2$ and $\mathbf{c}\in[H^{-1/2}(\partial D_i)]^2$, respectively. Let $\widetilde{\mathbf{e}}\in[H^{-1/2}(\partial\Omega)]^2$ stand for the zero extension of $\mathbf{e}$ to the entire boundary $\partial\Omega$. Take $\widetilde{H_{jl}^\alpha},\widetilde{K_{jl}^\alpha},\widetilde{K_{jl}^{\prime\alpha}}$ and $\widetilde{L_{jl}^\alpha}$ as the boundary integral operators similar to $H_{jl}^\alpha,K_{jl}^\alpha,K_{jl}^{\prime\alpha}$ and L_{jl}^α for $j,l=1,2,3$, respectively. The integrals are defined on ∂D_i for $j=1,2$, on the boundary $\partial\Omega$ for the case $j=3$, and take values on the boundary ∂D_i for $l=1,2$, on the boundary $\partial\Omega$ for the case $l=3$. Then the operator M becomes a corresponding one $\widetilde{M}$.

The assumption on the Lamé constants ensures that the Navier equation is strongly elliptic. Therefore there exists positive and bounded below operators H_l^α: $[H^{-1/2}(\partial D_i)]^2\to[H^{1/2}(\partial D_i)]^2$ and $-L_l^\alpha:[H^{1/2}(\partial D_i)]^2\to[H^{-1/2}(\partial D_i)]^2$ for $l=1,2$, i.e.,

$$Re\langle H_l^\alpha\mathbf{p},\mathbf{p}\rangle\ge c\|\mathbf{p}\|^2_{[H^{-1/2}(\partial D_i)]^2}\quad\text{for}\ \ \mathbf{p}\in[H^{-1/2}(\partial D_i)]^2$$

and

$$Re\langle -L_l^{\alpha}\mathbf{p},\mathbf{p}\rangle \geq c\|\mathbf{p}\|^2_{[H^{1/2}(\partial D_i)]^2} \quad \text{for} \quad \mathbf{p}\in [H^{1/2}(\partial D_i)]^2,$$

such that $\widetilde{H_l^{\alpha}} := \widetilde{H_{ll}^{\alpha}} - H_l^{\alpha} : [H^{-1/2}(\partial D_i)]^2 \to [H^{1/2}(\partial D_i)]^2$ and $\widetilde{L_l^{\alpha}} := -\widetilde{L_{ll}^{\alpha}} + L_l^{\alpha} : [H^{1/2}(\partial D_i)]^2 \to [H^{-1/2}(\partial D_i)]^2$ are compact operators (see Chapter 7 in [10]). Here $\langle\cdot,\cdot\rangle$ denotes the duality pairing between $[H^{1/2}(\partial D_i)]^2$ and $[H^{-1/2}(\partial D_i)]^2$. The same result holds for the operator $\widetilde{H_{33}^{\alpha}}$, the corresponding positive and bounded below operator is denoted by $H_3^{\alpha} : [H^{-1/2}(\partial\Omega)]^2 \to [H^{1/2}(\partial\Omega)]^2$ and we adopt the notation $\widetilde{H_3^{\alpha}} := \widetilde{H_{33}^{\alpha}} - H_3^{\alpha}$.

Let K_l^{α} and $K_l^{'\alpha}$ defined as $\widetilde{K_{ll}^{\alpha}}$ and $\widetilde{K_{ll}^{'\alpha}}$ for $l=1,2$, respectively, with Hankel function replaced by $-\frac{1}{2\pi}\ln|x-y|$ in the fundamental solution $\Gamma_{\alpha}(\cdot,\cdot)$. Then $\widetilde{K_l^{\alpha}} := \widetilde{K_{ll}^{\alpha}} - K_l^{\alpha}$ and $\widetilde{K_l^{'\alpha}} := \widetilde{K_{ll}^{'\alpha}} - K_l^{'\alpha}$ are compact operators since their integral kernels are continuous [34].

Then the operator $\widetilde{M}$ can be rewritten in the form

$$\begin{aligned}\widetilde{M} &= \begin{bmatrix} H_1^e + H_1^i & -K_1^e - K_1^i & 0 & 0 \\ K_1^{'e} + K_1^{'i} & -L_1^e - L_1^i & 0 & 0 \\ 0 & 0 & H_2^i & 0 \\ 0 & 0 & 0 & H_3^e \end{bmatrix} + \begin{bmatrix} \widetilde{H_1^e} + \widetilde{H_1^i} & -\widetilde{K_1^e} - \widetilde{K_1^i} & -\widetilde{H_{21}^i} & \widetilde{H_{31}^e} \\ \widetilde{K_1^{'e}} + \widetilde{K_1^{'i}} & \widetilde{L_1^e} + \widetilde{L_1^i} & -\widetilde{K_{21}^{'i}} & \widetilde{K_{31}^{'e}} \\ -\widetilde{H_{12}^i} & \widetilde{K_{12}^i} & \widetilde{H_2^i} & 0 \\ \widetilde{H_{13}^e} & -\widetilde{K_{13}^e} & 0 & \widetilde{H_3^e} \end{bmatrix} \\ &=: \widetilde{M_0} + \widetilde{M_c}.\end{aligned}$$

Let

$$Y := [H^{-1/2}(\partial D_i)]^2 \times [H^{1/2}(\partial D_i)]^2 \times [H^{-1/2}(\partial D_i)]^2 \times [H^{-1/2}(\partial\Omega)]^2,$$

$$Y^* :=\in [H^{1/2}(\partial D_i)]^2 \times [H^{-1/2}(\partial D_i)]^2 \times [H^{1/2}(\partial D_i)]^2 \times [H^{1/2}(\partial\Omega)]^2.$$

We see that $\widetilde{M} : Y \to Y^*$ is a bounded operator. Moreover, we have for $\widetilde{\chi} := [\widetilde{\mathbf{a}},\widetilde{\mathbf{b}},\widetilde{\mathbf{c}},\widetilde{\mathbf{e}}]^{\top} \in Y$

$$\begin{aligned}\left(\widetilde{M_0}\widetilde{\chi},\widetilde{\chi}\right) &= \langle H_1^e\widetilde{\mathbf{a}},\widetilde{\mathbf{a}}\rangle + \langle H_1^i\widetilde{\mathbf{a}},\widetilde{\mathbf{a}}\rangle - \langle K_1^e\widetilde{\mathbf{b}},\widetilde{\mathbf{a}}\rangle - \langle K_1^i\widetilde{\mathbf{b}},\widetilde{\mathbf{a}}\rangle + \langle K_1^{'e}\widetilde{\mathbf{a}},\widetilde{\mathbf{b}}\rangle + \langle K_1^{'i}\widetilde{\mathbf{a}},\widetilde{\mathbf{b}}\rangle \\ &\quad - \langle L_1^e\widetilde{\mathbf{b}},\widetilde{\mathbf{b}}\rangle - \langle L_1^i\widetilde{\mathbf{b}},\widetilde{\mathbf{b}}\rangle + \langle H_2^i\widetilde{\mathbf{c}},\widetilde{\mathbf{c}}\rangle + \langle H_3^e\widetilde{\mathbf{e}},\widetilde{\mathbf{e}}\rangle. \end{aligned} \tag{2.6}$$

The real kernels of K_1^{α} and $K_1^{'\alpha}$ indicate that they are adjoint operators, which implies that

$$Re\Big[-\langle K_1^e\widetilde{\mathbf{b}},\widetilde{\mathbf{a}}\rangle - \langle K_1^i\widetilde{\mathbf{b}},\widetilde{\mathbf{a}}\rangle + \langle K_1^{'e}\widetilde{\mathbf{a}},\widetilde{\mathbf{b}}\rangle + \langle K_1^{'i}\widetilde{\mathbf{a}},\widetilde{\mathbf{b}}\rangle\Big] = 0.$$

Thus taking the real part of (2.6) we obtain that

$$Re\left(\widetilde{M_0}\widetilde{\chi},\widetilde{\chi}\right) \geq c\left(\|\widetilde{\mathbf{a}}\|^2_{[H^{-1/2}(\partial D_i)]^2} + \|\widetilde{\mathbf{b}}\|^2_{[H^{1/2}(\partial D_i)]^2} + \|\widetilde{\mathbf{c}}\|^2_{[H^{-1/2}(\partial D_i)]^2} + \|\widetilde{\mathbf{e}}\|^2_{[H^{-1/2}(\partial\Omega)]^2}\right),$$

which shows that $\widetilde{M_0}$ is coercive. Noting that $\widetilde{\chi} = [\widetilde{\mathbf{a}},\widetilde{\mathbf{b}},\widetilde{\mathbf{c}},\widetilde{\mathbf{e}}]^{\top}$ is the extension by zero of $\chi := [\mathbf{a},\mathbf{b},\mathbf{c},\mathbf{e}]^{\top} \in X$, we have the following for the restricted operator $\widetilde{M_{0r}} : X \to X^*$ of $\widetilde{M_0}$

$$Re\left(\widetilde{M_{0r}}\chi,\chi\right) = Re\left(\widetilde{M_0}\widetilde{\chi},\widetilde{\chi}\right),$$

which leads to the coercive property of $\widetilde{M}_{0r}$.

On the other hand, since $\widetilde{H_l^\alpha}$, $\widetilde{K_l^\alpha}$, $\widetilde{K_l'^\alpha}$ and $\widetilde{L_l^\alpha}$ are compact operators as stated above, the corresponding restricted operators still maintain compactness. In addition, the other restricted operators in $\widetilde{M}_c$ are compact due to the continuous kernels. We summarize that the restricted operator $\widetilde{M}_{cr}: X \to X^*$ of $\widetilde{M}_c$ is compact.

Therefore the operator $M: X \to X^*$ can be decomposed as the sum of a coercive part and a compact part $M = \widetilde{M}_{0r} + \widetilde{M}_{cr}$. Thus we complete the proof of this lemma. ◻

LEMMA 2.3. *The operator $M: X \to X^*$ is injective.*

Proof. Let $\chi := [\mathbf{a}, \mathbf{b}, \mathbf{c}, \mathbf{e}]^\top$ satisfy $M\chi = \mathbf{0}$, and we next prove $\chi = \mathbf{0}$.

Recall the potentials $\mathbf{u}, \mathbf{v}$ given by (2.3) and (2.4), respectively. The condition $M\chi = \mathbf{0}$ means that $(\mathbf{u}, \mathbf{v})$ solves problem (2.1) with homogeneous boundary value, and Lemma 2.1 (the uniqueness result) shows that $\mathbf{u} = \mathbf{0}$ in D_e and $\mathbf{v} = \mathbf{0}$ in D_i. Therefore, the jump relation for $T_e\mathbf{u}$ crossing the boundary $\Gamma := \Sigma \backslash \Gamma_2$ implies

$$\mathbf{e}|_\Gamma = T_e\mathbf{u}|_{\Gamma^-} - T_e\mathbf{u}|_{\Gamma^+} = \mathbf{0}.$$

So the density $\mathbf{e}$ belongs to $[\widetilde{H}^{-1/2}(\Gamma_2)]^2$ and the potential $\mathbf{u}$ is essentially defined on the boundary Γ_2. In this case, the fourth equation in (2.5) indicates

$$H_{12}^e\mathbf{a} - K_{12}^e\mathbf{b} + H_{22}^e\mathbf{e} = \mathbf{0}. \tag{2.7}$$

Now, redefine the potentials $\mathbf{u}, \mathbf{v}$ still the same forms as before and let $\mathbf{u}$ defined in the domain D_i and $\mathbf{v}$ defined in the domain D_e. Then $\mathbf{u}$ and $\mathbf{v}$ satisfy the Navier equation in corresponding region.

Using the jump relations of the single-and-double layer potentials, we reduce that on the boundary Γ_1

$$(\mathbf{v} - \mathbf{u})|_{\Gamma_1} = -(H_{11}^i + H_{11}^e)\mathbf{a} + (K_{11}^i + K_{11}^e)\mathbf{b} + H_{21}^i\mathbf{c} - H_{31}^e\mathbf{e}$$

and

$$(T_i\mathbf{v} - T_e\mathbf{u})|_{\Gamma_1} = -(K_{11}'^i + K_{11}'^e)\mathbf{a} + (L_{11}^i + L_{11}^e)\mathbf{b} + K_{21}'^i\mathbf{c} - K_{31}'^e\mathbf{e}.$$

A similar calculation yields that on the boundary Γ_2

$$\mathbf{v}|_{\Gamma_2^+} = -H_{12}^i\mathbf{a} + K_{12}^i\mathbf{b} + H_{22}^i\mathbf{c},$$

and

$$\mathbf{u}|_{\Gamma_2^-} = H_{12}^e\mathbf{a} - K_{12}^e\mathbf{b} + H_{22}^e\mathbf{e}.$$

We arrive at the following problem from the fact $M\chi = \mathbf{0}$ and relation (2.7)

$$\begin{cases} \Delta_e^*\mathbf{u} + \rho_e\omega^2\mathbf{u} = \mathbf{0} & \text{in } D_i, \\ \Delta_i^*\mathbf{v} + \rho_i\omega^2\mathbf{v} = \mathbf{0} & \text{in } \mathbb{R}^2\backslash\overline{D}_i, \\ \mathbf{v} - \mathbf{u} = \mathbf{0} & \text{on } \Gamma_1, \\ T_i\mathbf{v} - T_e\mathbf{u} = \mathbf{0} & \text{on } \Gamma_1, \\ \mathbf{v} = \mathbf{0} & \text{on } \Gamma_2^+, \\ \mathbf{u} = \mathbf{0} & \text{on } \Gamma_2^-, \end{cases} \tag{2.8}$$

where $\mathbf{v}$ satisfies the Kupradze radiation condition. By a very similar derivation as Lemma 2.1, it is easy to verify that problem (2.8) possess a unique trivial solution.

We conclude from foregoing analysis that the following potentials $\mathbf{u}$ and $\mathbf{v}$ both equal to zero.

$$\mathbf{u}(\mathbf{x})=\int_{\Gamma_1}\Big\{\Gamma_e(\mathbf{x},\mathbf{y})\mathbf{a}(\mathbf{y})-[T_{e,\mathbf{y}}\Gamma_e(\mathbf{x},\mathbf{y})]^\top\mathbf{b}(\mathbf{y})\Big\}ds(\mathbf{y})+\int_{\Gamma_2}\Gamma_e(\mathbf{x},\mathbf{y})\mathbf{e}(\mathbf{y})ds(\mathbf{y}),\ \mathbf{x}\in\mathbb{R}^2\backslash\partial D_i,$$

$$\mathbf{v}(\mathbf{x})=\int_{\Gamma_1}\Big\{[T_{i,\mathbf{y}}\Gamma_i(\mathbf{x},\mathbf{y})]^\top\mathbf{b}(\mathbf{y})-\Gamma_i(\mathbf{x},\mathbf{y})\mathbf{a}(\mathbf{y})\Big\}ds(\mathbf{y})+\int_{\Gamma_2}\Gamma_i(\mathbf{x},\mathbf{y})\mathbf{c}(\mathbf{y})ds(\mathbf{y}),\ \mathbf{x}\in\mathbb{R}^2\backslash\partial D_i.$$

Hence, we obtain

$$\mathbf{a}=T_i\mathbf{v}|_{\Gamma_1^+}-T_i\mathbf{v}|_{\Gamma_1^-}=\mathbf{0},\qquad \mathbf{b}=\mathbf{v}|_{\Gamma_1^+}-\mathbf{v}|_{\Gamma_1^-}=\mathbf{0},$$

$$\mathbf{c}=T_i\mathbf{v}|_{\Gamma_2^-}-T_i\mathbf{v}|_{\Gamma_2^+}=\mathbf{0},\qquad \mathbf{e}=T_e\mathbf{u}|_{\Gamma_2^-}-T_e\mathbf{u}|_{\Gamma_2^+}=\mathbf{0},$$

which ends the proof of this lemma. ◻

From Lemma 2.2 and Lemma 2.3 we derive that $M:X\to X^*$ is invertible owing to the Fredholm theorem. Thus the solution of problem (2.1) has the specific representation (2.3) and (2.4) in term of the densities $\mathbf{a}$, $\mathbf{b}$, $\mathbf{c}$ and $\mathbf{e}$ determined by $M^{-1}[\mathbf{f},\mathbf{g},\mathbf{0},\mathbf{h}]^\top$. This assertion together with Lemma 2.1 imply the well posedness of the direct scattering problem (2.1), which is stated as follows.

THEOREM 2.1. *Assume that* $\mathbf{f}\in[H^{1/2}(\Gamma_1)]^2$, $\mathbf{g}\in[H^{-1/2}(\Gamma_1)]^2$ *and* $\mathbf{h}\in[H^{1/2}(\Sigma)]^2$, *then there exists a unique solution* $(\mathbf{u},\mathbf{v})\in[H^1_{loc}(D_e)]^2\times[H^1(D_i)]^2$ *to problem (2.1) satisfying*

$$\|\mathbf{u}\|_{[H^1(B_r\cap D_e)]^2}+\|\mathbf{v}\|_{[H^1(D_i)]^2}\le c\Big(\|\mathbf{f}\|_{[H^{1/2}(\Gamma_1)]^2}+\|\mathbf{g}\|_{[H^{-1/2}(\Gamma_1)]^2}+\|\mathbf{h}\|_{[H^{1/2}(\Sigma)]^2}\Big),$$

where B_r *is a disk of radius* r *containing* $D_i\cup\Sigma$ *and* c *is a constant depending on* r *but not on* $\mathbf{f},\mathbf{g}$ *and* $\mathbf{h}$.

3. The linear sampling method for IP

This part is devoted to the inverse problem **IP** by using the linear sampling method. Some of the arguments depend heavily on the conclusions of the paper [33].

We begin with the elastic Herglotz wavefunction with density $\tau=(\tau_p,\tau_s)\in[L^2(\mathbb{S})]^2$ defined by

$$\mathbf{v}_\tau(\mathbf{x})=e^{-i\pi/4}\int_{\mathbb{S}}\Big\{\sqrt{\frac{k_{p,e}}{\omega}}e^{ik_{p,e}\mathbf{d}\cdot\mathbf{x}}\mathbf{d}\tau_p(\mathbf{d})+\sqrt{\frac{k_{s,e}}{\omega}}e^{ik_{s,e}\mathbf{d}\cdot\mathbf{x}}\mathbf{d}^\perp\tau_s(\mathbf{d})\Big\}ds(\mathbf{d}),\quad \mathbf{x}\in\mathbb{R}^2. \tag{3.1}$$

The Hilbert space $[L^2(\mathbb{S})]^2$ in this paper is equipped with the inner product

$$\langle\mathbf{g},\mathbf{h}\rangle=\frac{\omega}{k_{p,e}}\int_{\mathbb{S}}g_p\overline{h_p}ds+\frac{\omega}{k_{s,e}}\int_{\mathbb{S}}g_s\overline{h_s}ds,\quad \mathbf{g},\mathbf{h}\in[L^2(\mathbb{S})]^2.$$

Denote by W the subset of elastic Herglotz wavefunctions satisfying

$$W:=\Big\{\mathbf{v}_\tau:\mathbf{v}_\tau|_{\Gamma_2}=\mathbf{0}\Big\}.$$

REMARK 3.1. In this part, the elastic Herglotz wavefunction $\mathbf{v}_\tau$ is assumed to belongs to the subset W, which may be due to the unusual scattering problem. This special incident waves ensure that the linear sampling can be applied to the inverse problem **IP** as we will see later.

We set a hypothetical condition throughout this paper. Let's consider the following problem for $\mathbf{f}\in[H^{1/2}(\Gamma_1)]^2$

$$\begin{cases} \Delta_\alpha^*\mathbf{v}^f+\rho_\alpha\omega^2\mathbf{v}^f &=\mathbf{0} \quad \text{in } D_i,\\ \mathbf{v}^f &=\mathbf{f} \quad \text{on } \Gamma_1,\\ \mathbf{v}^f &=\mathbf{0} \quad \text{on } \Gamma_2. \end{cases} \tag{3.2}$$

Assumption 1. For $\alpha=i,e$, the circular frequency ω is not a Dirichlet eigenvalue of problem (3.2), i.e., problem (3.2) with boundary data $\mathbf{f}=\mathbf{0}$ has only trivial solution for such ω.

Next we introduce two function spaces related closely to elastic Herglotz wavefunctions. The space $U(D_i)$ is given by

$$U(D_i):=\Big\{\mathbf{u}\in[H^1(D_i)]^2:\ \Delta_e^*\mathbf{u}+\rho_e\omega^2\mathbf{u}=\mathbf{0}\text{ in } D_i,\ \mathbf{u}=\mathbf{0}\text{ on }\Gamma_2\Big\}.$$

It is well known that the vector elastic Herglotz wavefunctions are dense in the space of solutions to the Navier equation in D_i with respect to the $[H^1(D_i)]^2$-norm [36]. Of course, the subset W is dense in the subspace $U(D_i)$ of $[H^1(D_i)]^2$, and we denote it by $H(D_i)$. Hence it holds that $\overline{H(D_i)}=U(D_i)$. We consequently define a subspace of $[H^{1/2}(\Gamma_1)]^2\times[H^{-1/2}(\Gamma_1)]^2$ by

$$\mathbb{H}(\Gamma_1):=\Big\{(\mathbf{u}|_{\Gamma_1},T_e\mathbf{u}|_{\Gamma_1}):\mathbf{u}\in\overline{H(D_i)}\Big\}. \tag{3.3}$$

Based on the analysis in Theorem 3.1 of the paper [37], one can obtain that every function in $[H^{1/2}(\Gamma_3)]^2$ can be approximated by the trace of an elastic Herglotz wavefunction with respect to the $[H^{1/2}(\Gamma_3)]^2$ norm. Now define the subspace of $[H^{1/2}(\Gamma_3)]^2$

$$\mathbb{H}(\Gamma_3)=\Big\{\mathbf{u}:\mathbf{u}\in[H^{1/2}(\Gamma_3)]^2,\mathbf{u}|_{\Gamma_2}=\mathbf{0}\Big\}, \tag{3.4}$$

then the subset W is dense in $\mathbb{H}(\Gamma_3)$ with respect to $[H^{1/2}(\Gamma_3)]^2$-norm, i.e.,

$$\mathbb{H}(\Gamma_3):=\overline{\Big\{\mathbf{v}_\tau|_{\Gamma_3}:\mathbf{v}_\tau\in H(D_i)\Big\}}. \tag{3.5}$$

By an analogous argument as Lemma 4.3 in [33], we have that $\mathbb{H}(\Gamma_1)$ is a closed subset of $[H^{1/2}(\Gamma_1)]^2\times[H^{-1/2}(\Gamma_1)]^2$ if **Assumption 1** is satisfied.

Furthermore, it holds

LEMMA 3.1. *$\mathbb{H}(\Gamma_1)\times\mathbb{H}(\Gamma_3)$ is a closed subset of $[H^{1/2}(\Gamma_1)]^2\times[H^{-1/2}(\Gamma_1)]^2\times[H^{1/2}(\Gamma_3)]^2$ if **Assumption 1** is satisfied and thus is a Banach space.*

Denote by $\mathcal{H}:[L^2(\mathbb{S})]^2\to[H^{1/2}(\Gamma_1)]^2\times[H^{-1/2}(\Gamma_1)]^2\times[H^{1/2}(\Gamma_3)]^2$ the Herglotz wave operator which takes values of the Herglotz wavefunction $\mathbf{v}_\tau$ on the boundaries, that is

$$\mathcal{H}\tau=(\mathbf{v}_\tau|_{\Gamma_1},T_e\mathbf{v}_\tau|_{\Gamma_1},\mathbf{v}_\tau|_{\Gamma_3}),\ \text{for } \mathbf{v}_\tau\in H(D_i). \tag{3.6}$$

The definitions of the spaces $\mathbb{H}(\Gamma_1)$ and $\mathbb{H}(\Gamma_3)$ imply that

LEMMA 3.2. *The operator $\mathcal{H}:[L^2(\mathbb{S})]^2\to\mathbb{H}(\Gamma_1)\times\mathbb{H}(\Gamma_3)$ has dense range.*

According to the superposition principle [34], the elastic far field operator F: $[L^2(\mathbb{S})]^2 \to [L^2(\mathbb{S})]^2$ can be defined by

$$(F\tau)(\hat{\mathbf{x}}) = e^{-i\pi/4}\int_{\mathbb{S}}\left\{\sqrt{\frac{k_{p,e}}{\omega}}\mathbf{u}^\infty(\hat{\mathbf{x}},\mathbf{d};\mathbf{d})\tau_p(\mathbf{d}) + \sqrt{\frac{k_{s,e}}{\omega}}\mathbf{u}^\infty(\hat{\mathbf{x}},\mathbf{d};\mathbf{d}^\perp)\tau_s(\mathbf{d})\right\}ds(\mathbf{d}), \quad \hat{\mathbf{x}} \in \mathbb{S}, \tag{3.7}$$

where $\mathbf{u}^\infty$ is the far field pattern of the scattered field $\mathbf{u}$ to the problem (1.1)–(1.5). It is exactly the far field pattern of the resulted scattered field inspired by the incidence of Herglotz wavefunction.

We now consider the problem (2.1) with boundary data $(\mathbf{f},\mathbf{g},\mathbf{h}) \in [H^{1/2}(\Gamma_1)]^2 \times [H^{-1/2}(\Gamma_1)]^2 \times \mathbb{H}(\Gamma_3)$. The well posedness of this problem defines an operator G mapping the boundary data $(\mathbf{f},\mathbf{g},\mathbf{h})$ to the far field pattern $\mathbf{u}^\infty \in [L^2(\mathbb{S})]^2$, i.e.,

$$G(\mathbf{f},\mathbf{g},\mathbf{h})(\hat{\mathbf{x}}) = \mathbf{u}^\infty(\hat{\mathbf{x}}), \quad \hat{\mathbf{x}} \in \mathbb{S}. \tag{3.8}$$

Then it follows that

$$F\tau = -G(\mathcal{H}\tau). \tag{3.9}$$

Next, we focus our attention on the study of the operators F and G. To this end, we introduce the so-called interior transmission problem, which is closely related to the injectivity of the far field operator F. The interior transmission problem corresponding to the scattering problem (2.1) reads: for given $\mathbf{f} \in [H^{1/2}(\Gamma_1)]^2$, $\mathbf{g} \in [H^{-1/2}(\Gamma_1)]^2$, find $\mathbf{w},\mathbf{v} \in [H^1(D_i)]^2$ such that

$$\begin{cases} \Delta_e^*\mathbf{w} + \rho_e\omega^2\mathbf{w} = \mathbf{0} & \text{in } D_i, \\ \Delta_i^*\mathbf{v} + \rho_i\omega^2\mathbf{v} = \mathbf{0} & \text{in } D_i, \\ \mathbf{w} - \mathbf{v} = \mathbf{f} & \text{on } \Gamma_1, \\ T_e\mathbf{w} - T_i\mathbf{v} = \mathbf{g} & \text{on } \Gamma_1, \\ \mathbf{v} = \mathbf{0} & \text{on } \Gamma_2, \\ \mathbf{w} = \mathbf{0} & \text{on } \Gamma_2. \end{cases} \tag{3.10}$$

One can treat this problem following the basic idea of paper [35]. A similar problem has been investigated in [33] for the case of acoustic scattering. The values of ω for which a non-trivial solution to the homogeneous interior transmission problem exists are called transmission eigenvalues. Here, we assume, but without any proof, that the set of transmission eigenvalues ω is discrete.

LEMMA 3.3. *Assume that ω is not the transmission eigenvalue, then the far field operator F is injective with dense range.*

Proof. As is presented in [20], we can examine that the adjoint $F^*: [L^2(\mathbb{S})]^2 \to [L^2(\mathbb{S})]^2$ of the far field operator F is $F^*\tau = \overline{RFR\overline{\tau}}, \tau \in [L^2(\mathbb{S})]^2$, where $(R\mathbf{f})(\mathbf{d}) := \mathbf{f}(-\mathbf{d})$ is the reflection operator. In view of this relation, the injectivity of F implies the denseness of its range. Hence we just need to show that F is injective.

Now consider the solution $(\mathbf{u},\mathbf{v})$ of the scattering problem (1.1)–(1.5) for the incidence of Herglotz wavefunction $\mathbf{v}_\tau$. Assume that $F\tau = \mathbf{0}$ with $\tau \neq \mathbf{0}$, that is, the far field pattern of scattered field $\mathbf{u}$ is zero. Then Rellich's lemma gives that $\mathbf{u} = \mathbf{0}$ in the domain D_e and thus $\mathbf{v}_\tau|_\Sigma = \mathbf{0}$ from the boundary condition, which indicates that $\mathbf{v}_\tau|_{\Gamma_2} = \mathbf{0}$. Consequently, the non-zero function pair $(\mathbf{v},\mathbf{v}_\tau)$ satisfies the homogeneous interior transmission problem (3.10), which is contrary to the assumption. The proof is then completed. ∎

We next turn to explore the properties of the operator G and the discussion follows the basic ideas in [33]. It is different from the case of impenetrable scatterers, the operator G is no longer injective. In fact, the well posedness of the problem (3.2) defines the Dirichlet-to-Neumann operator $\Lambda:[H^{1/2}(\Gamma_1)]^2\to[H^{-1/2}(\Gamma_1)]^2$ by

$$\Lambda\mathbf{f}=T_\alpha\mathbf{f}|_{\Gamma_1}$$

. Following the proof procedure in Theorem 4.1 of paper [33], one can prove the result below with necessary modifications.

Lemma 3.4. *The kernel space of G is given by $\mathcal{N}(G)=\left\{(\mathbf{f},\Lambda\mathbf{f},\mathbf{0}):\mathbf{f}\in[H^{1/2}(\Gamma_1)]^2\right\}$ under **Assumption 1**.*

However, by restricting the domain of definition, we will show that the operator G becomes injective. Let G_0 be the restriction of G to the space $\mathbb{H}(\Gamma_1)\times\mathbb{H}(\Gamma_3)$.

Lemma 3.5. *The operator G_0 is compact, injective and has dense range in $[L^2(\mathbb{S})]^2$ if ω is not a transmission eigenvalue.*

Proof. Since G_0 can be decomposed into the product of a bounded operator, which maps the boundary data $(\mathbf{f},\mathbf{g},\mathbf{h})\in\mathbb{H}(\Gamma_1)\times\mathbb{H}(\Gamma_3)$ to the scattering solution $(\mathbf{u},\mathbf{v})$ of problem (2.1), and a compact operator, which maps the radiating solution $\mathbf{u}$ to its far field pattern, we observe that G_0 is compact.

To prove the injectivity of G_0, let $G_0(\mathbf{f},\mathbf{g},\mathbf{h})=\mathbf{0}$, in other words, the far field pattern of the radiating solution $\mathbf{u}$ is zero. Then $\mathbf{u}$ vanishes in D_e by the Rellich's lemma, and the trace theorem shows that $\mathbf{u}|_{\Gamma_1}\underline{=\mathbf{0},T_e}\mathbf{u}|_{\Gamma_1}=\mathbf{0}$ and $\mathbf{h}=\mathbf{u}|_{\Gamma_3}=\mathbf{0}$. By the definition of the space $\mathbb{H}(\Gamma_1)$, there exists $\mathbf{w}\in\underline{H(D_i)}$ such that $\mathbf{f}=\mathbf{w}|_{\Gamma_1},\mathbf{g}=T_e\mathbf{w}|_{\Gamma_1}$. We conclude that $(\mathbf{w},\mathbf{v})$ satisfies the homogeneous interior transmission problem (3.10). It follows $\mathbf{w}=\mathbf{0},\mathbf{v}=\mathbf{0}$ from the assumption that ω is not a transmission eigenvalue, whence $\mathbf{f}=\mathbf{0},\mathbf{g}=\mathbf{0}$. So the injectivity of G_0 is proved.

Notice that the range of the far field operator F is included in the range of G, from Lemma 3.3 we know that G possesses dense range if ω is not a transmission eigenvalue. In order to prove the denseness of G_0, it is enough to demonstrate $\mathcal{R}(G)\subset\mathcal{R}(G_0)$. Let $\mathbf{u}^\infty\in\mathcal{R}(G)$ with $\mathbf{u}^\infty$ being the far field pattern of the radiating part $\mathbf{u}$ of the solution pair $(\mathbf{u},\mathbf{v})$. Consider the unique solution $(\mathbf{w},\mathbf{v})$ of interior transmission problem with boundary data $(\mathbf{u}|_{\Gamma_1},T_e\mathbf{u}|_{\Gamma_1})$, it follows immediately that $(\mathbf{u},\mathbf{v})$ solves problem (2.1) with boundary data $(\mathbf{w}|_{\Gamma_1},T_e\mathbf{w}|_{\Gamma_1},,\mathbf{u}|_{\Gamma_3})\in\mathbb{H}(\Gamma_1)\times\mathbb{H}(\Gamma_3)$. As a result, $\mathbf{u}^\infty\in\mathcal{R}(G_0)$, thus complete the proof. □

The reconstruction algorithm of the linear sampling method is based on solving the far field equation

$$(F\tau)(\hat{\mathbf{x}})=\Phi^\infty(\hat{\mathbf{x}})\quad\text{for } \tau\in[L^2(\mathbb{S})]^2,\ \hat{\mathbf{x}}\in\mathbb{S}, \tag{3.11}$$

where Φ^∞ is the far field pattern of the following potential

$$\Phi(\mathbf{x})=\int_{L_1}\Gamma_e(\mathbf{x},\mathbf{y})\phi(\mathbf{y})ds(\mathbf{y})+\int_{L_1}[T_{e,y}\Gamma_e(\mathbf{x},\mathbf{y})]^\top\varphi(\mathbf{y})ds(\mathbf{y}) + \int_{L_2}\Gamma_e(\mathbf{x},\mathbf{y})\psi(\mathbf{y})ds(\mathbf{y}),\quad \mathbf{x}\in D_e \tag{3.12}$$

with (ϕ,φ,ψ) being any functions in the space $[\widetilde{H}^{-1/2}(\Gamma)]^2\times[\widetilde{H}^{1/2}(\Gamma)]^2\times[\widetilde{H}^{-1/2}(L)]^2$ such that $\Phi|_{\Gamma_2}=\mathbf{0}$. Here L_1,L_2 are any two smooth non intersecting arcs without cusps such that $L_1\cap L_2=\emptyset$.

In Equation (3.11), the measured data is stored in the far field operator F, and Φ^∞ is selected as the test function for any two open curves. However, why can this information be used to find out the scatterers. The following result gives the answer by noting the relation $F=-G_0\mathcal{H}$ between F and G_0.

LEMMA 3.6. *Assume that ω is not a transmission eigenvalue, then the far field pattern $\Phi^\infty(\hat{\mathbf{x}})$ of the potential $\Phi(\mathbf{x})$ given by (3.12) is in the range of G_0 if and only if $L_1\subset D_i$ and $L_2\subset\Gamma_3$.*

Proof. If $L_1\subset D_i$ and $L_2\subset\Gamma_3$, consider the solution $(\mathbf{w},\mathbf{v})$ of the interior transmission problem (3.10) with boundary data $\mathbf{f}=\mathbf{\Phi}|_{\Gamma_1},\mathbf{g}=T_e\mathbf{\Phi}|_{\Gamma_1}$. We observe that $(\mathbf{v},\Phi)$ solves problem (2.1) with boundary data $(\mathbf{w}|_{\Gamma_1},T_e\mathbf{w}|_{\Gamma_1},\mathbf{\Phi}|_{\Gamma_3})\in\mathbb{H}(\Gamma_1)\times\mathbb{H}(\Gamma_3)$. It follows that $\Phi^\infty(\hat{\mathbf{x}})\in\mathcal{R}(G_0)$ from the definition of the operator G_0.

Now we assume that at least one of the situation: $L_1\subset D_i$ and $L_2\subset\Gamma_3$, is not satisfied. Without loss of generality, let $L_1\not\subset D_i$ and $L_2\subset\Gamma_3$, and on the contrary, assume that $\Phi^\infty(\hat{\mathbf{x}})$ belongs to $\mathcal{R}(G_0)$. Then there exists $\mathbf{w}\in\overline{H(D_i)}$ and $\mathbf{h}\in\mathbb{H}(\Gamma_3)$ such that

$$G_0(\mathbf{w}|_{\Gamma_1},T_e\mathbf{w}|_{\Gamma_1},\mathbf{h})=\Phi^\infty.$$

Let $(\mathbf{u},\mathbf{v})$ be the solution to problem (2.1) with boundary data $(\mathbf{w}|_{\Gamma_1},T_e\mathbf{w}|_{\Gamma_1},\mathbf{h})$, then we have $\mathbf{u}^\infty=\Phi^\infty$ by the injectivity of G_0. Rellich's lemma and unique continuation principle yield that $\mathbf{u}$ equals to Φ in the domain $D_e\backslash\overline{L}_1$, which contradicts to the fact that $\mathbf{u}$ belongs to $H^1_{loc}(D_e)$ but Φ does not, because of the singularity of Φ on the curve L_1.

For the case of $L_1\subset D_i$ and $L_2\not\subset\Gamma_3$ or $L_1\not\subset D_i$ and $L_2\not\subset\Gamma_3$, we can also derive a contradiction by a similar discussion as above. The proof is completed. □

The foregoing analysis leads to the mathematical foundation of the linear sampling method, which shows the relation between the behavior of solution to (3.11) and the test curves L_1 and L_2. When $L_1\subset D_i$ and $L_2\subset\Gamma_3$ the norm of the solution τ is bounded, otherwise, its becomes large and this phenomenon exactly reports the location of the scatterers. So we can say that the behavior of the approximate solution to the far field Equation (3.11) plays as an indicator function to characterize the mixed scatterer.

THEOREM 3.1. *Assume that ω is not a transmission eigenvalue and **Assumption 1** is satisfied. Then for the far field Equation (3.11) the following holds:*

(1) If $L_1\subset D_i$ and $L_2\subset\Gamma_3$, for every $\epsilon>0$ there exists a solution $\tau^\epsilon_{L_1,L_2}\in[L^2(\mathbb{S})]^2$ satisfying

$$\|F\tau^\epsilon_{L_1,L_2}+\Phi^\infty_{L_1,L_2}\|_{[L^2(\mathbb{S})]^2}<\epsilon.$$

(2) If $L_1\not\subset D_i$ or $L_2\not\subset\Gamma_3$, then for every $\epsilon>0$ and $\delta>0$, there exists a function $\tau^{\epsilon,\delta}_{L_1,L_2}\in[L^2(\mathbb{S})]^2$ such that

$$\|F\tau^{\epsilon,\delta}_{L_1,L_2}+\Phi^\infty_{L_1,L_2}\|_{[L^2(\mathbb{S})]^2}<\epsilon+\delta,$$

and

$$\lim_{\delta\to 0}\|\tau^{\epsilon,\delta}_{L_1,L_2}\|_{[L^2(\mathbb{S})]^2}=\infty.$$

Proof.

(1) For the case $L_1 \subset D_i$ and $L_2 \subset \Gamma_3$, there exists a solution $(\mathbf{w},\mathbf{v})$ of the interior transmission problem (3.10) with boundary data $\mathbf{f}=\mathbf{\Phi}|_{\Gamma_1}, \mathbf{g}=T_e\mathbf{\Phi}|_{\Gamma_1}$. We observe that $(\mathbf{v},\Phi)$ solves problem (2.1) with boundary data $(\mathbf{w}|_{\Gamma_1}, T_e\mathbf{w}|_{\Gamma_1}, \mathbf{\Phi}|_{\Gamma_3}) \in \mathbb{H}(\Gamma_1)\times\mathbb{H}(\Gamma_3)$. From Lemma 3.2, for every $\epsilon>0$ there exists a function $\tau^{\epsilon}_{L_1,L_2} \in [L^2(\mathbb{S})]^2$ such that

$$\|\mathcal{H}\tau^{\epsilon}_{L_1,L_2} - (\mathbf{w}|_{\Gamma_1}, T_e\mathbf{w}|_{\Gamma_1}, \mathbf{\Phi}|_{\Gamma_3})\|_{[H^{1/2}(\Gamma_1)]^2\times[H^{-1/2}(\Gamma_1)]^2\times[H^{1/2}(\Gamma_3)]^2} < \epsilon/\|G_0\|, \tag{3.13}$$

since the operator G_0 is bounded and we have

$$\|G_0(\mathcal{H}\tau^{\epsilon}_{L_1,L_2}) - G_0(\mathbf{w}|_{\Gamma_1}, T_e\mathbf{w}|_{\Gamma_1}, \mathbf{\Phi}|_{\Gamma_3})\|_{[L^2(\mathbb{S})]^2} < \epsilon.$$

Hence we obtain

$$\|F\tau^{\epsilon}_{L_1,L_2} + \Phi^{\infty}_{L_1,L_2}\|_{[L^2(\mathbb{S})]^2} < \epsilon$$

due to $F=-G_0\mathcal{H}$ and $G_0(\mathbf{w}|_{\Gamma_1}, T_e\mathbf{w}|_{\Gamma_1}, \mathbf{\Phi}|_{\Gamma_3}) = \Phi^{\infty}_{L_1,L_2}$. Noting that $\mathbf{w}$ and $v_{\tau^{\epsilon}_{L_1,L_2}}$ belong to $\overline{H(D_i)}$, the inequality (3.13) implies that $v_{\tau^{\epsilon}_{L_1,L_2}}$ converges to $\mathbf{w}$ in the space $[H^1(D_i)]^2$ as $\epsilon\to 0$. As a result the norm $\|\tau^{\epsilon}_{L_1,L_2}\|_{[L^2(\mathbb{S})]^2}$ is bounded.

(2) Next, we assume that $L_1 \not\subset D_i$ or $L_2 \not\subset \Gamma_3$. In this case, Lemma 3.6 makes us know that $\Phi^{\infty}_{L_1,L_2}$ is not in the range of G_0, but Lemma 3.5 shows that G_0 is compact, injective and with dense range in $[L^2(\mathbb{S})]^2$. Hence, for every $\delta>0$ we can construct an unique Tikhonov regularized solution $(\mathbf{f}^{\rho},\mathbf{g}^{\rho},\mathbf{h}^{\rho}) \in \mathbb{H}(\Gamma_1)\times\mathbb{H}(\Gamma_3)$ of equation $G_0(\mathbf{f},\mathbf{g},\mathbf{h}) = \Phi^{\infty}_{L_1,L_2}$, such that

$$\|G_0(\mathbf{f}^{\rho},\mathbf{g}^{\rho},\mathbf{h}^{\rho}) - \Phi^{\infty}_{L_1,L_2}\|_{[L^2(\mathbb{S})]^2} < \delta,$$

where ρ is the regularization parameter (chosen by a regularization strategy, e.g., the Morozov's discrepancy principle). Then we obtain

$$\|(\mathbf{f}^{\rho},\mathbf{g}^{\rho},\mathbf{h}^{\rho})\|_{[H^{1/2}(\Gamma_1)]^2\times[H^{-1/2}(\Gamma_1)]^2\times[H^{1/2}(\Gamma_3)]^2} \to \infty \text{ as } \rho\to 0.$$

By Theorem 3.2, $\mathcal{H}$ has dense range, thus for $\epsilon>0$ sufficiently small there exists $\tau^{\epsilon,\rho}_{L_1,L_2}$ such that

$$\|\mathcal{H}\tau^{\epsilon,\rho}_{L_1,L_2} - (\mathbf{f}^{\rho},\mathbf{g}^{\rho},\mathbf{h}^{\rho})\|_{[H^{1/2}(\Gamma_1)]^2\times[H^{-1/2}(\Gamma_1)]^2\times[H^{1/2}(\Gamma_3)]^2} < \epsilon/\|G_0\|.$$

Combining the above two equations we obtain that for every $\epsilon>0$ and $\delta>0$ there exists $\tau^{\epsilon,\rho}_{L_1,L_2} \in [L^2(\mathbb{S})]^2$ such that

$$\begin{aligned}\|F\tau^{\epsilon,\rho}_{L_1,L_2} + \Phi^{\infty}_{L_1,L_2}\|_{[L^2(\mathbb{S})]^2} &= \|G_0(\mathcal{H}\tau^{\epsilon,\rho}_{L_1,L_2}) - \Phi^{\infty}_{L_1,L_2}\|_{[L^2(\mathbb{S})]^2}\\ &\le \|G_0(\mathcal{H}\tau^{\epsilon,\rho}_{L_1,L_2}) - G_0(\mathbf{f}^{\rho},\mathbf{g}^{\rho},\mathbf{h}^{\rho})\|_{[L^2(\mathbb{S})]^2}\\ &\quad + \|G_0(\mathbf{f}^{\rho},\mathbf{g}^{\rho},\mathbf{h}^{\rho}) - \Phi^{\infty}_{L_1,L_2}\|_{[L^2(\mathbb{S})]^2}\\ &< \epsilon+\delta.\end{aligned}$$

Since $\lim_{\delta\to 0}\rho(\delta)=0$, it arrives at

$$\lim_{\delta\to 0}\|(\mathbf{f}^{\rho},\mathbf{g}^{\rho},\mathbf{h}^{\rho})\|_{[H^{1/2}(\Gamma_1)]^2\times[H^{-1/2}(\Gamma_1)]^2\times[H^{1/2}(\Gamma_3)]^2} \to \infty.$$

So we deduce that $\lim_{\delta\to 0}\|\mathcal{H}\tau^{\epsilon,\rho}_{L_1,L_2}\|_{[H^{1/2}(\Gamma_1)]^2\times[H^{-1/2}(\Gamma_1)]^2\times[H^{1/2}(\Gamma_3)]^2} \to \infty$ and thus $\lim_{\delta\to 0}\|\tau^{\epsilon,\rho}_{L_1,L_2}|_{[L^2(\mathbb{S})]^2} \to \infty$ due to the boundedness of $\mathcal{H}$. The proof is completed.

∎

4. The numerical examples

In this part, we present some numerical experiments to verify the validity of the established linear sampling method in two dimensions. In all examples we assume that the host elastic medium has Lamé constants $\lambda_e = 1, \mu_e = 2$, the included medium has Lamé constants $\lambda_i = 1.5, \mu_i = 2.5$ and the mass densities take value $\rho_e = \rho_i = 1$.

The scheme of the numerical experiment for the linear sampling method is described in the following steps.

FIG. 4.1. *The exact objects: the shape of circle arc and line (left), the shape of semi-ellipse and line (right)*

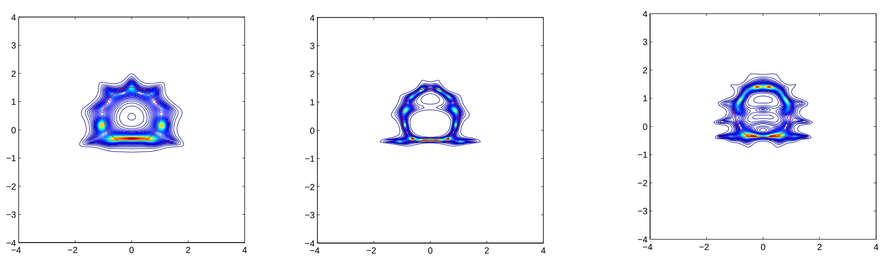

a. $\omega = 3$ b. $\omega = 4$ c. $\omega = 6$

FIG. 4.2. *Reconstruction of the circle arc and line for* $\mathbf{q} = [0,1]^\top$*, noise level=1%, with different circular frequencies* ω*.*

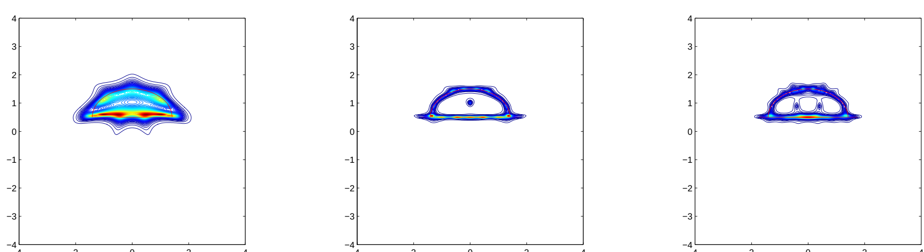

a. $\omega = 3$ b. $\omega = 6$ c. $\omega = 8$

FIG. 4.3. *Reconstruction of the semi-ellipse and line for* $\mathbf{q} = [0,1]^\top$*, noise level=1%, with different circular frequencies* ω*.*

Firstly, the forward data is generated synthetically by solving the direct scattering problem (1.1)∼ (1.5), where the collocation and quadrature approaches [38, 39] are used to treat the numerical solution procedure. Then the far field data of the elastic

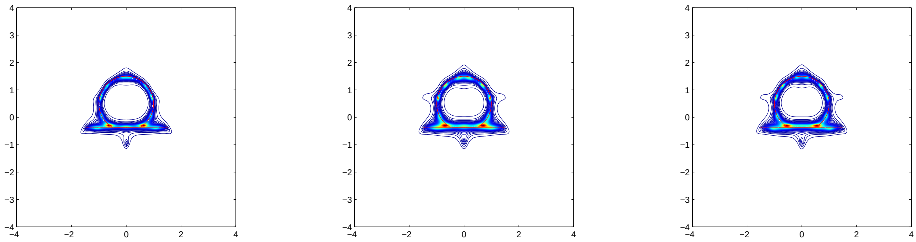

a. no noise b. 5% noise c. 10% noise

FIG. 4.4. *Reconstruction of the circle arc and line for* $\omega=4$, $\mathbf{q}=[1,0]^\top$ *with different noise levels.*

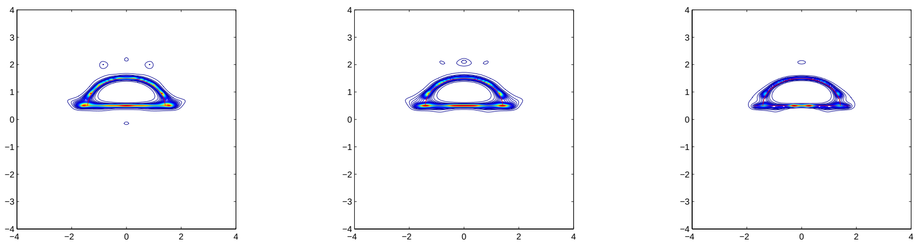

a. no noise b. 5% noise c. 15% noise

FIG. 4.5. *Reconstruction of the semi-ellipse and line for* $\omega=4$, $\mathbf{q}=[0,1]^\top$ *with different noise levels.*

scattering field can be calculated through the combined potential (2.3), in which, the far field patterns of the single-and double-layer potentials are computed by

$$(H_{j,a}^\infty \mathbf{g})(\hat{\mathbf{x}}) = \beta_a \int_{\Gamma_j} J_a(\hat{\mathbf{x}})\mathbf{g}(\mathbf{y}) e^{-ik_{a,e}\hat{\mathbf{x}}\cdot\mathbf{y}} ds(\mathbf{y})$$

and

$$(K_{j,a}^\infty \mathbf{g})(\hat{\mathbf{x}}) = \gamma_a \int_{\Gamma_j} J_a(\hat{\mathbf{x}}) B(\hat{\mathbf{x}},\mathbf{y})\mathbf{g}(\mathbf{y}) e^{-ik_{a,e}\hat{\mathbf{x}}\cdot\mathbf{y}} ds(\mathbf{y}),$$

respectively, with the coefficients

$$\beta_p = \frac{1}{2\mu_e+\lambda_e}\frac{e^{i\pi/4}}{\sqrt{8\pi k_{p,e}}}, \quad \beta_s = \frac{1}{\mu_e}\frac{e^{i\pi/4}}{\sqrt{8\pi k_{s,e}}},$$

$$\gamma_p = \frac{e^{-i\pi/4}}{2\mu_e+\lambda_e}\sqrt{\frac{k_{p,e}}{8\pi}}, \quad \gamma_s = \frac{e^{-i\pi/4}}{\mu_e}\sqrt{\frac{k_{s,e}}{8\pi}},$$

and the matrices $J_p = \hat{\mathbf{x}}\hat{\mathbf{x}}^\top/|\hat{\mathbf{x}}|^2$, $J_s = I - J_p$ and

$$B(\hat{\mathbf{x}},\mathbf{y}) = \lambda_e \hat{\mathbf{x}}\mathbf{n}(\mathbf{y})^\top + \mu_e \mathbf{n}(\mathbf{y})\hat{\mathbf{x}}^\top + \mu_e \mathbf{n}(\mathbf{y})\cdot\hat{\mathbf{x}} I.$$

The second step involves dealing with far field Equation (3.11). For N incident directions $\mathbf{d}_l = (\cos(2\pi l/N), \sin(2\pi l/N))^\top, l = 1,\ldots,N$, and for N observation directions $\hat{\mathbf{x}}_m = (\cos(2\pi m/N), \sin(2\pi m/N))^\top, m = 1,\ldots,N$, the limited data of the far field patterns $\mathbf{u}^\infty(\hat{\mathbf{x}},\mathbf{d};\mathbf{d})$ and $\mathbf{u}^\infty(\hat{\mathbf{x}},\mathbf{d};\mathbf{d}^\perp)$ for N plane compressional and shear waves, respectively,

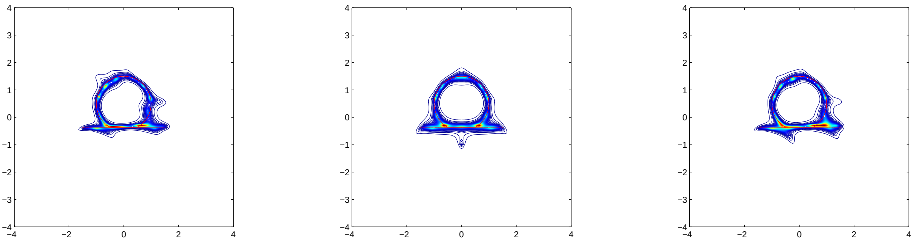

a. $\mathbf{q}=[\sqrt{2}/2,\sqrt{2}/2]^\top$ b. $\mathbf{q}=[-1,0]^\top$ c. $\mathbf{q}=[-\sqrt{3}/2,-1/2]^\top$

FIG. 4.6. *Reconstruction of the circle arc and line for $\omega=4$, noise level = 1% with different polarization directions* $\mathbf{q}$.

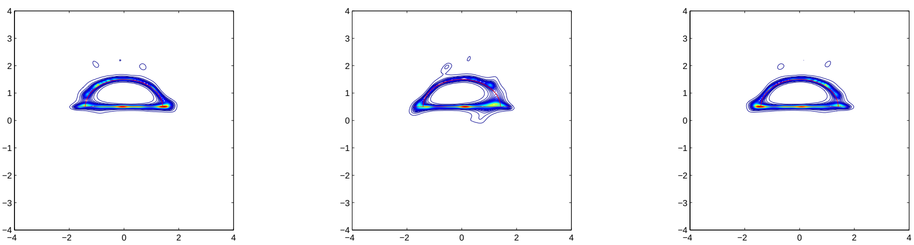

a. $\mathbf{q}=[1/2,\sqrt{3}/2]^\top$ b. $\mathbf{q}=[-\sqrt{(3)}/2,1/2]^\top$ c. $\mathbf{q}=[1/2,-\sqrt{3}/2]^\top$

FIG. 4.7. *Reconstruction of the semi-ellipse and line for $\omega=4$, noise level = 1% with different polarization directions* $\mathbf{q}$.

are obtained and the discretized far field operator F is approximated by matrix $F_N\in\mathbb{C}^{2N\times 2N}$ given by

$$F_N=\frac{2\pi}{N}e^{-i\pi/4}\begin{bmatrix}\sqrt{\frac{k_p}{\omega}}u_p^\infty(\hat{\mathbf{x}}_m,\mathbf{d}_l;\mathbf{d}_l) & \sqrt{\frac{k_s}{\omega}}u_p^\infty(\hat{\mathbf{x}}_m,\mathbf{d}_l;\mathbf{d}_l^\perp)\\ \sqrt{\frac{k_p}{\omega}}u_s^\infty(\hat{\mathbf{x}}_m,\mathbf{d}_l;\mathbf{d}_l) & \sqrt{\frac{k_s}{\omega}}u_s^\infty(\hat{\mathbf{x}}_m,\mathbf{d}_l;\mathbf{d}_l^\perp)\end{bmatrix}.$$

Another aspect concerns the test function $\Phi^\infty(\hat{\mathbf{x}})$ appearing on the right hand side of the Equation (3.11), which is the far field pattern of the combined potential Φ given by (3.12) and integrating on the test curve L_1 and L_2. It is hard to make the curve located in the actual boundary Γ_1 and the crack Σ. Furthermore, the assumption that $\Phi=0$ on Γ_2 can not be ensured since the location of Γ_2 is unknown. As a result, the numerical experiment here is not completely consistent with the previous theoretical analysis. So, we take the second best and choose the far field pattern $(\Gamma^\infty_{p,e}(\hat{\mathbf{x}},\mathbf{z};\mathbf{p}),\Gamma^\infty_{s,e}(\hat{\mathbf{x}},\mathbf{z};\mathbf{p}))$ of an elastic point source $\Gamma_e(\mathbf{x},\mathbf{z})\cdot\mathbf{p}$ in $\mathbf{z}\in\mathbb{R}^2$ with the polarization direction $\mathbf{p}\in\mathbb{S}$ as the test function. We think it will not fundamentally affect the numerical experiment because the numerical integration on the test curve needs to be discretized into the values at some points. This treatment has been adopted by Cakoni [37] to recovery cracks in acoustic scattering. Thus the test function can be approximated by a column vector $\Phi_N^\infty\in\mathbb{C}^{2N}$ given by

$$\Phi_N^\infty=\begin{bmatrix}\frac{1}{2\mu+\lambda}\frac{e^{i\pi/4}}{\sqrt{8\pi k_p}}e^{-ik_p\hat{\mathbf{x}}_m\cdot\mathbf{z}}\hat{\mathbf{x}}_m\cdot\mathbf{p}\\ \frac{1}{\mu}\frac{e^{i\pi/4}}{\sqrt{8\pi k_s}}e^{-ik_s\hat{\mathbf{x}}_m\cdot\mathbf{z}}\hat{\mathbf{x}}_m^\perp\cdot\mathbf{p}\end{bmatrix}.$$

Due to the ill posedness of the far field equation, the Tikhonov regularization method is employed to solve the normal equation

$$\rho\tau + F_N^{\delta *} F_N^{\delta}\tau = F_N^{\delta *}\Phi_N^{\infty}(\cdot,\mathbf{z},\mathbf{p})$$

with regularization parameter ρ, where δ is the error level of the far field operator, i.e., $\|F_N^{\delta} - F_N\|_{L^2(\mathbb{S})} < \delta$. For each given ϵ and δ, the regularization parameter ρ is chosen by the generalized Morozov's discrepancy principle, i.e., $\|F_N^{\delta}\tau(\cdot,\mathbf{z},\mathbf{p}) - \Phi_N^{\infty}(\cdot,\mathbf{z},\mathbf{p})\|_{L^2(\mathbb{S})} = \epsilon + \delta\|\tau(\cdot,\mathbf{z},\mathbf{p})\|_{L^2(\mathbb{S})}$. Assume $\epsilon \ll \delta$ and thus can be ignored in above identity. We can obtain the solution $\tau(\cdot,\mathbf{z},\mathbf{p})$ by using a singular system $\{\sigma_j,\phi_j,\psi_j\}_{j=1}^{2N}$ for the operator F_N^{δ} as

$$\tau(\cdot,\mathbf{z},\mathbf{p}) = \sum_{j}^{2N} \frac{\sigma_j}{\rho+\sigma_j^2}(\Phi_N^{\infty}(\cdot,\mathbf{z},\mathbf{p}),\psi_j)_{L^2(\mathbb{S})}\phi_j,$$

where ρ is the root of the monotonically increasing function

$$f(\rho) := \sum_{j}^{2N} \frac{\rho^2 - \delta^2\sigma_j^2}{(\rho+\sigma_j^2)^2}|(\Phi_N^{\infty}(\cdot,\mathbf{z},\mathbf{p}),\psi_j)_{L^2(\mathbb{S})}|^2.$$

The last step is to choose a region covering the expected obstacle, then for each sampling point $\mathbf{z}$ lying in this region, the norm of $\|\tau(\cdot,\mathbf{z},\mathbf{p})\|_{L^2(\mathbb{S})}$ is calculated and we plot $1/\|\tau(\cdot,\mathbf{z},\mathbf{p})\|_{L^2(\mathbb{S})}$ with 100 contour lines at fixed polarization $\mathbf{p}$. The value of which becomes large when $\mathbf{z}$ lies in the exact boundary Γ_1 and the crack Σ and thereby can be used as an indicator function to characterize the combined elastic scatterer. In the reconstruction, the far-field data are given for 40 incident directions and 40 observation directions equally distributed on the unit circle and we use a grid of 161×161 equally spaced sampling points on the rectangle $[-4,4]\times[-4,4]$.

We show the reconstruction results in the following two examples. Consider the circle arc

$$\Gamma_1 := \left\{\left(\cos\frac{\pi s}{3}, \frac{1}{2} + \sin\frac{\pi s}{3}\right) : -1 \le s \le 4\right\}$$

lying on the line

$$\Sigma := \left\{(-\frac{\sqrt{3}}{2}\cot\frac{\pi s}{6}, -\frac{\sqrt{3}}{2} + \frac{1}{2}) : 1 \le s \le 5\right\}$$

in Figure 4.2, 4.4 and 4.6, and consider the semi-ellipse

$$\Gamma_1' := \left\{\left(\sqrt{2}\cos\pi s, \sin\pi s + \frac{1}{2}\right) : 0 \le s \le 1\right\}$$

lying on the line

$$\Sigma' := \left\{(-\cot\frac{\pi s}{6}, \frac{1}{2}) : 1 \le s \le 5\right\}$$

in Figure 4.3, 4.5 and 4.7. In all the examples, we show the reconstructions by using the MATLAB routine contour $(\mathbf{z}_x, \mathbf{z}_y, 1/\|\tau(\cdot,\mathbf{z},\mathbf{p})\|_{L^2(\mathbb{S})})$.

The numerical experiments show the viability of our method. In addition, we observe that:

(1) The reconstructed scatterer is stable for noise, the quality of the reconstructions increases with decreasing error level.

(2) The polarization direction $\mathbf{p}$ has a certain influence on the experiments, since the norm of the indicator function $\|\tau(\cdot,\mathbf{z},\mathbf{p})\|_{L^2(\mathbb{S})}$ is related to the polarization direction, different polarization direction implies different norm.

(3) The reaction to the circular frequency ω is sensitive in the numerical examples and the experimental effect is just relatively good for $\omega=4,5,6$, this phenomenon may be related to the size of the scatterer.

REFERENCES

[1] P.M. Morse and H. Feshbach, *Methods of Theoretical Physics vols I, II*, New York: McGraw-Hill, 1953.

[2] V.D. Kupradze, *Potential Methods in the Theory of Elasticity*, Israel Program for Scientific Translations, Jerusalem, 1965.

[3] K. Kiriaki and V. Sevroglou, *Integral equations methods in obstacle elastic scattering*, Bull. Greek Math. Soc., 45:57–69, 2001.

[4] C.J.S. Alves and R. Kress, *On the far-field operator in elastic obstacle scattering*, IMA J. Appl. Math., 67:1–21, 2002.

[5] T. Ha-Duong, *On the boundary integral equations for the crack opening displacement of flat cracks*, Integral Eq. Oper. Theory, 15:427–453, 1992.

[6] R. Kress, *Inverse elastic scattering from a crack*, Inverse Problems, 12:667–684, 1996.

[7] E.P. Stephan, *Boundary Integral Equations for crack Problems in* $\mathbb{R}^3$, Integral Eq. Oper. Theory, 10:236–257, 1987.

[8] M. Costabel and E.P. Stephan, *Integral equations for transmission problems in linear elasticity*, J. integral Eq. Appl., 2:211–223, 1990.

[9] P. Hahner and G. Hsiao, *Uniqueness theorems in inverse obstacle scattering of elastic waves*, Inverse Problems, 9:525–534, 1993.

[10] W. McLean, *Strongly Elliptic Systems and Boundary Integral Equations*, Cambridge: Cambridge University Press, 2000.

[11] C.E. Athanasiadis, D. Natroshvili, V. Sevroglou, and I.G. Stratis, *A boundary integral equations approach for mixed impedance problems in elasticity*, J. Integral Eq. Appl., 23:183–222, 2011.

[12] D. Colton and A. Kirsch, *A simple method for solving inverse scattering problems in the resonance region*, Inverse Problems, 12:383–393, 1996.

[13] T. Arens and A. Lechleiter, *The linear sampling method revisited*, J. Integral Eq. Appl., 21:179–202, 2009.

[14] F. Cakoni and D. Colton, *On the mathematic basis of the linear sampling method*, Georg. Math. J., 10:411–425, 2003.

[15] F. Cakoni and D. Colton, *A Qualitative Approach to Inverse Scattering Theory*, AMS, Springer, 188, 2014.

[16] T. Arens and A. Lechleiter, *Indicator functions for shape reconstruction related to the linear sampling method*, SIAM J. Imaging Sciences, 8:513–535, 2015.

[17] L. Audibert and H. Haddar, *A generalized formulation of the linear sampling method with exact characterization of targets in terms of farfield measurements*, Inverse Problems, 30:035011, 2014.

[18] T. Arens, *Linear sampling methods for 2D inverse elastic wave scattering*, Inverse Problems, 17:1445–1464, 2001.

[19] D. Gintides and K. Kiriaki, *The far-field equations in linear elasticityan inversion scheme*, Z. Angew. Math. Mech., 81:305–316, 2001.

[20] A. Charalambopoulos, D. Gintides, and K. Kiriaki, *The linear sampling method for the transmission problem in three-dimensional linear elasticity*, Inverse Problems, 18:547–558, 2002.

[21] A. Charalambopoulos, D. Gintides, and K. Kiriakie, *The linear sampling method for non-absorbing penetrable elastic bodies*, Inverse Problems, 19:549–561, 2003.

[22] K. Anagnostopoulos and A. Charalambopoulos, *The linear sampling method for the transmission problem in 2D anisotropic elasticity*, Inverse Problems, 22:553–577, 2006.

[23] S. Nintcheu Fata and B. Guzina, *A linear sampling method for near-field inverse problems in elastodynamics*, Inverse Problems, 20:713–736, 2004.

[24] P. Monk and V. Selgas, *Near field sampling type methods for the inverse fluidsolid interaction problem*, Inverse Problems and Imaging, 5:465–483, 2011.

[25] N. Grinberg and A. Kirsch, *The factorization method for obstacles with a priori separated sound-soft and sound-hard parts*, Math. Comput. Simul., 66:267–279, 2004.

[26] M. Martin, *Multiple Scattering, Encyclopedia of Mathematics and its Applications*, Cambridge: Cambridge University Press, 107, 2006.

[27] F. Hassen, J. Liu, and R. Potthast, *On source analysis by wave splitting with applications in inverse scattering of multiple obstacles*, J. Comput. Math., 25:266–281, 2007.

[28] M. Ganesh and S. Hawkins, *An efficient algorithm for simulating scattering by a large number of two dimensional particles*, ANZIAM J. Electron. Suppl., 52:C139–C155, 2010.

[29] J. Cheng, J. Liu, G. Nakamura, and S. Wang, *Recovery of multiple obstacles by probe mehtod*, Quart. Appl. Math., 67:221–247, 2009.

[30] A. Kirsch and X. Liu, *Direct and inverse acoustic scattering by a mixed-type scatterer*, Inverse Problems, 29:065005, 2013.

[31] X. Liu, *The factorization method for scatterers with different physical properties*, Dis. Cont. Dyn. Sys. S, 8:563–577, 2017.

[32] J. Guo, Q. Wu, and G. Yan, *The linear sampling method for a mixed scattering problem*, Inverse Probl. Sci. En., 24:1–20, 2014.

[33] J. Guo and G. Yan, *The inverse scattering problem for partially penetrable obstacles*, Applicable Analysis, 97(1), 2018.

[34] D. Colton and R. Kress, *Inverse Acoustic and Electromagnetic Scattering Theory 3rd ed*, Springer Verlag: Berlin, 2013.

[35] A. Charalambopoulos, *On the interior transmission problem in nondissipative, inhomogeneous, anisotropic elasticity*, J. Elasticity, 67:149–170, 2002.

[36] T. Arens, *An approximation property of elastic Herglotz wavefunctions and its application in the linear sampling method*, J. Inv. Ill-Posed Problems, 11:219–233, 2003.

[37] F. Cakoni and D. Colton, *The linear sampling method for cracks*, Inverse Problems, 19:279–295, 2003.

[38] R. Chapko, *On the numerical solution of a boundary value problem in the plane elasticity for a double-connected domain*, Math. Comput. Simul., 66:425–438, 2004.

[39] R. Chapko, R. Kress, and L. Monch, *On the numerical solution of a hypersingular integral equation for elastic scattering from a planar crack*, IMA J. Numer. Anal., 20:601–619, 2000.